

IMPACT OF TWO TROPICAL CYCLONES ON THE RADIO ATMOSPHERICS OBSERVED USING VLF RECEIVERS

BAKUL DAS^{1,6}, ARNAB SEN^{2,6}, KHEYALI BARMAN^{1,6}, SUJAY PAL^{3,6}, PRABIR KR.
HALDAR^{1,6*}, SUSHANTA K. MONDAL⁴ AND SUBRATA K. MIDYA⁵

¹Department of Physics, Cooch Behar PanchananBarma University, Panchanan Nagar, Cooch Behar,
WB-736101, India

²Department of Education in Science and Mathematics, NERIE, NCERT, Meghalaya-79310, India

³Department of Physics, Srikrishna College, Nadia, WB-741502, India

⁴Department of Physics, SidhoKanhoBirsra University, Purulia, WB-723104, India

⁵Department of Atmospheric Sciences, University of Calcutta, WB-700019, India

⁶Near-Earth Space & Atmospheric Observatory, West Bengal, India.

*E-mail: prabirkrhaldar@gmail.com

Received

Abstract. The response of electric field intensity of VLF radio atmospherics during two tropical cyclones Fani (May 2019) and Amphan (May 2020) has been presented in this paper. VLF radio atmospherics (or VLF sferics) received at Coochbehar (CHB) and Kolkata (CUB) at three discrete frequencies (4 kHz, 7 kHz, and 9 kHz) showed clear amplitude anomalies with respect to the reference level during the two cyclonic storms. This is explained using the electrical structure and distribution of cloud-to-ground lightning associated with the cyclones. Effects of ‘local lightning’ and ‘distant lightning’ have been identified for both the CUB and CHB receivers. Field intensity of VLF sferics at CUB station was found to get enhanced for both types of lightning events. But the intensity of VLF sferics at CHB station was found to be reduced for ‘distant lightning’ and enhanced for ‘local lightning’, possible reasons of which are also explained.

Keywords: Radio atmospherics; VLF sferics; Tropical Cyclones; Upper atmosphere; Lightning.

1. INTRODUCTION

Lightning emits the strongest natural electromagnetic radiation in the Earth's atmosphere within the frequency range from a few Hz to 10 GHz [1,2]. Radio atmospherics or lightning sferics are the broadband electromagnetic emissions that are generated during a lightning discharge. These emissions are mostly concentrated in the Very Low Frequency (VLF) band having frequency 3-30 kHz and called VLF sferics. The sferics can propagate through the Earth-Ionosphere Wave Guide (EIWG) up to thousands of kilometers with attenuation coefficients of 2-3 dB/Mm [3,4]. Since the acceleration of charged particles within the lightning return stroke produces the VLF sferics, they are important to contain information about the lightning generation process [5]. VLF sferics can be received directly or indirectly by a suitable receiving system from the ground. On average, at any moment 50 lightning occur per second globally. The total field intensity of the VLF sferics, is the result of those individual lightning flashes. The arrival of lightning sferics may occur directly or by reflection from the D-region of the ionosphere [6]. The amplitude of VLF sferics shows diurnal variation depending on the location of the receivers [7,8]. The diurnal nature of VLF electric field atmospherics may not always show 'Carnegie curve' in some areas of the globe depending on the atmospheric weather at the receiving location [9,10]. The diurnal variations can also be modified by natural phenomena like solar events, lightning thunderstorms, or even by earthquakes [11]. The study of VLF sferics during severe meteorological conditions such as tropical cyclones attracts special attention in the tropical region [12]. VLF radio atmospherics, during a tropical cyclone associated with intense lightning activity, show sharp variation in their field intensity. For example, the radio atmospherics in the ELF (Extremely Low Frequency) and VLF band show a fluctuation during Tropical Cyclone 'Roanu' in May, 2016 [13]. In another work it is observed that, VLF sferics during the cyclone 'Aila' and reported sudden enhancement in the field intensity of VLF sferics at 3 kHz and 9 kHz which were much higher than normal thunderstorms [14].

Tropical cyclones not only affect the propagation of natural VLF signals originating from the lightning discharges but also affect the propagation of fixed-frequency navigational transmitter signals as evidence of modification of ionospheric plasma during the intense cyclone period. The effects on the ionosphere during cyclones are thought to be mainly caused by two mechanisms; the electromagnetic channel due to lightning and the acoustic channel due to atmospheric gravity waves (AGWs). Lightning is found to be present in the eye wall and in the rain-bands of TCs [15]. Wang et al. (2018) studied the variation of lightning density at different stages and in different parts of TCs. They found the presence of lightning in the rain-bands throughout the total duration of

cyclone/hurricane, but in the inner core region lightning intensity was at a peak during tropical depression and super typhoon stage [16]. Pan et al. (2014) analyzed lightning activity during the typhoons in the Northwest Pacific Ocean and found good correlation between typhoons sustained wind speed and accumulated lightning flashes over a region of radius 600 km from typhoon center. A lightning generated radio signal may extend up to 10 GHz with peak energy at 5-10 kHz [17]. This peak emission of lightning VLF sferics electric field is sufficient to produce, the required D-region ionospheric ionization voltage, thus causing ionospheric changes and corresponding atmospheric optical emission of lightning spark [18].

The AGWs generated from the cyclonic system are found to couple the lower atmosphere with the upper atmosphere [19-22]. These investigations were mainly based on the GPS-TEC, radar, ionosonde data. For example, Perevalova et al. 2010 investigated ionospheric variation associated with cyclones using GPS-TEC data and found perturbations in several ionospheric parameters due to the cyclones. Bishop et al. 2006 reported a large velocity variation of F-region plasma using radar, ionosonde, and GPS data. Impacts of tropical cyclone (TC) on the lower ionosphere (60-100 km) were also studied deeply using VLF transmitter signals and reported in recent times [19]. VLF transmitter signals are an efficient tool to investigate the generation of gravity waves and diagnose their properties [23-26]. A strong correlation between AGWs in shorter wavelengths detected by VLF signals and cyclone intensity was reported recently by Pal et al. 2020 associated with the tropical cyclone Fani of 2019 over the Indian Ocean. VLF transmitter signals respond to cyclone induced ionospheric conductivity modulation depending on the relative position of the signal propagation paths and the cyclone path [27]. Das et al. 2020 also approximated the spatial dimension of the disturbed D-region ionosphere by simulating the VLF signal variation associated with the tropical cyclone Fani over the Indian Ocean [28]. Deviation of terminator time during tropical cyclone is analyzed for the first in a very recent study [29].

In this paper, we have presented an analysis of electric field intensity of VLF sferics at lower band (4-10 kHz) as received by two ingeniously developed VLF receivers associated with the two tropical cyclones 'Fani' of 2019 and 'Amphan' of 2020 over the North Indian Ocean region. The 'Fani' was in the category of Extremely Severe Cyclonic Storm (ESCS), and the 'Amphan' was in the category of Super Cyclonic Storm (SuCS). We show how VLF sferics respond differently at two places with respect to cloud-to-ground lightning activity associated with the cyclonic storms which also indicate the electrical structures of the cyclones. In the next section, we present experimental arrangements for data collection and the methodology for analysis of VLF sferics. In the third section, we show the results of the observations and lastly, we make conclusions.

2. EXPERIMENTAL ARRANGEMENT AND DATA

We monitor electric field amplitude of VLF signals of several navigational transmitters e.g. VTX of India (18.2 kHz), NWC of Australia (19.8 kHz), JJI of Japan (22.2 kHz) along with the electric field intensity sferics signals at 4 kHz, 7 kHz and 9 kHz from two low latitude stations Cooch Behar (CHB) and Kolkata (CUB). The stations CHB (26.35° N, 89.45° E) and CUB (22.570° N, 88.260° E) are approximately 450 km apart from each other. Reception of these frequencies is done by a stable receiving system which includes an active E-field antenna fed to a two stage band pass pre-amplifier with a gain factor 21. Signal is carried to the indoor recording unit by a RG-54 coaxial cable. For continuous logging of the E-field amplitudes with a sampling rate 4 Hz we use Spectrum lab V2.0 software (<https://www.qsl.net>). Internal computer clock have been synchronized with fixed internet time server.

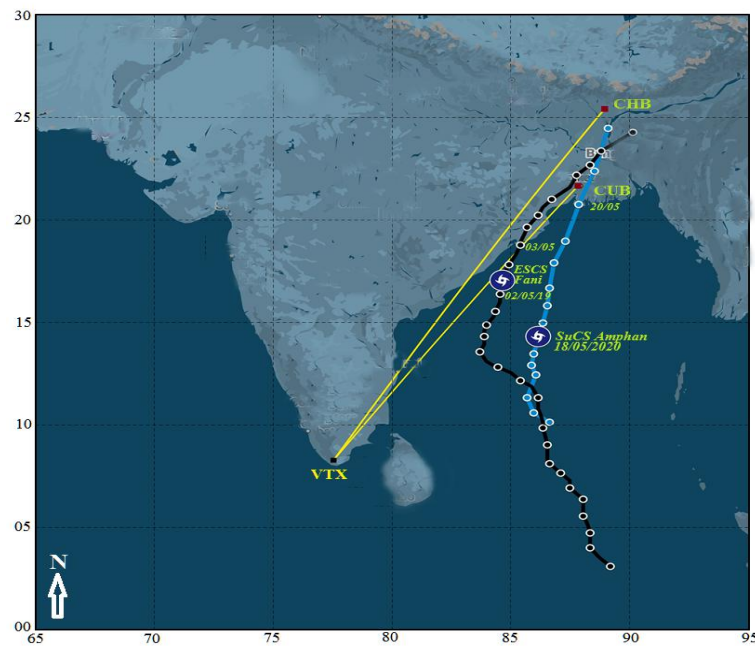


Fig. 1 - Geographical map showing the locations of VLF transmitter VTX (Black Square), receivers CHB (Maroon Square) and CUB (Maroon Square) including VTX-CHB and VTX-CUB Great Circle Paths (yellow line). Black curve (with black dots) showing track of ESCS Fani and Blue curve (with blue dots) presents the track of SuCS Amphan. Violet circulating symbols showing respectively the positions the maximum intensity of the cyclones.

Geographic location of the receiving stations and transmitter-receiver Great Circle

Paths (GCPs) are shown in Figure 1. We monitor VTX transmitter round the clock since 2018. The tracks of two cyclones are also drawn in the map with black (Fani) and Blue (Amphan) lines. Positions of the cyclones with highest sustained wind speed (115 kt for Fani and 130 kt for Amphan) have been marked by violet circulating symbols.

Here in this paper we focus on the cyclone associated lightning events and their impacts on the VLF radio atmospherics during these two tropical cyclones. To check the lightning events associated with the cyclones, the total lightning data are taken from the Earth Networks Total Lightning Network (ENTLN). ENTLN detects of in-cloud (IC) and cloud-to-ground (CG) flashes using sensors that operate in a frequency band spanning the VLF, LF, MF, and HF ranges [30]. We have considered only the CG flashes since these are the strongest source of VLF sferics. Relevant data related to the cyclones are obtained from the website of the India Meteorological Department (IMD).

3. RESULTS AND DISCUSSION

3.1 CASE OF FANI

Here we present the VLF sferics signals at three frequencies received at both CHB and CUB during the ESCS Fani of 2019. Fig. 2a shows the time series of the electric field amplitudes at 4 kHz (upper panel), 7 kHz (middle panel), and 9 kHz (lower panel) signals from 26 April to 8 May 2019 for the CHB station. The red dotted curve in each panel shows the average electric field variation obtained from the mean of 7 days signal before the depression formed. The two red solid horizontal lines in each panel show the $\pm 3\sigma$ range, and the blue solid curves are the actual field amplitude of the sferics. Minimum in diurnal variation is observed around 4 UT (9:30 LT) and maximum is observed around 15-16 UT (20:30-21:30 LT). The cyclonic storm Fani converted to ESCS on 30 April with maximum intensity on 02 May. Accordingly, we can see in Fig. 2a, signal amplitudes deviated by more than -3σ from 01 May onward and had maximum deviations on 02 May 2019 at all the sferics amplitudes. The signal strength increased from the minimum value from the same day (02 May) onward. The cyclone crossed the coastal region of Puri, India on 03 May and moved toward North. The lightning associated with the cyclone was located generally far (~ 1000 - 2000 km) from the receiver at CHB on 1-2 May, which caused more ionospheric propagation of the sferics signal to CHB. The distribution of cloud-to-ground (CG) lightning flash associated with Fani over the entire affected region is shown in Fig. 3 for 01 May (0-24 UT), 02 May (6-12 UT, 12-18 UT, and 18-24 UT), 03 May (0-24 UT), and

04 May (0-24 UT) respectively. The eye of the cyclone is clearly visible on 02 May when lightning were grouped in to 6 hourly intervals and the lightning occurred in the vicinity of the eye were distinguished by the red circle. Also the lightning activity was found to be concentrated near the eye and along the spiral band of the cyclone Fani. Lightning activity was most over the Ocean on 02 May and the same was increased over the land after landfall on 03 May. The minimum in the sferics amplitude on 02 May was caused by the ionospheric propagation effects resulting in a destructive modal interference among the propagating waveguide modes from the 'distant lightning'.

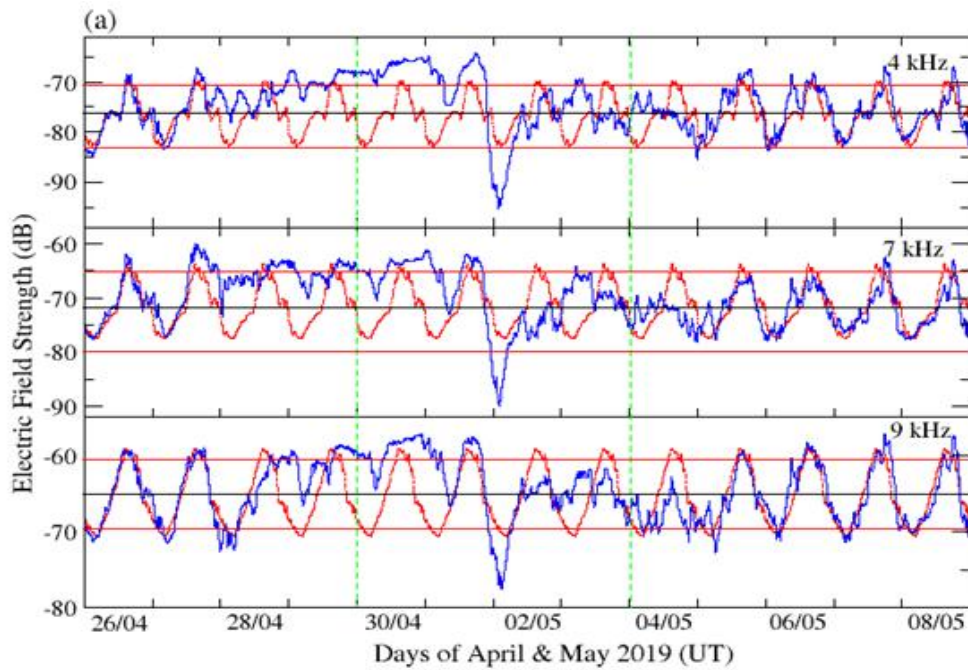


Fig. 2: Each panel represents the VLF sferics amplitude (dB) from 26/04/2019 to 10/05/2019 received at CHB (solid blue curve), compared with the mean amplitude (red dotted curve). Two red solid horizontal lines represent $\pm 3\sigma$ range. Upper panel represents the sferics amplitude at 4 kHz, middle and lower panel are the VLF sferics of 7 kHz and 9 kHz respectively. Two green dashed vertical lines indicate the period of ESCS Fani.

Fig. 4a shows the CG lightning flash count per day within 200 km around the receivers CUB (upper panel) and CHB (lower panel). We call these 'local lightning' to separate it from the 'distant lightning' for which the sferics signal traveled a long distance (in this case $\sim 1000-3000$ km) through the EIWG before

being received at CUB or CHB. Unfortunately, we do not have data before 01 May 2019. As can be seen from the case of CHB (Fig. 4 and also from Fig.3) that there was more ‘local lightning’ on 01 May. As a result, the receiver recorded direct waves from the ‘local lightning’ that occurred around the CHB and caused an increase in sferics amplitude above $+3\sigma$ level.

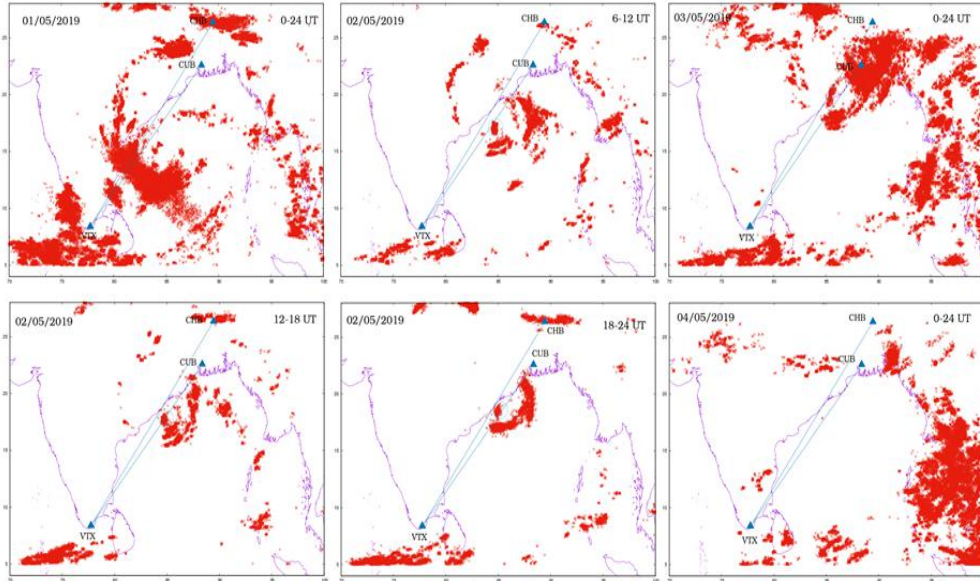


Fig. 3: Distribution of Cloud-to-Ground (including both +CG and -CG) lightning flashes at several stages of the ESCS Fani from 01 May to 04 May. Lightning enclosed by the small circle were occurred in the vicinity of the eye. The eye-wall, inner rain band and outer rain band are clearly visible when grouped into 6 hourly intervals such as shown for 02 May.

Similarly, on 29 April and 30 April, ‘local lightning’ occurred near to the receiver at CHB (IMD storm project report) associated with afternoon thunderstorms which caused the receiver to record direct waves from the lightning instead of ionospheric propagation and resulted in an increase of amplitude above $+3\sigma$ level. The lightning associated with cyclone on 03 May were closer to the receiver at CHB as can be seen from Fig. 3 and thus received more direct sferics waves from the lightning which also caused increase in signal amplitude.

Fig. 5 shows the variation of sferics amplitudes at the same frequencies for the Kolkata (CUB) station. In general, minimum in diurnal variation was observed around $\sim 4-5$ UT (9:30-10:30 LT) and maximum was observed around 12-14 UT (17:30-19:30 LT) for any normal day at CUB. Here the amplitudes increased from 30 April 2019 and stayed above $+3\sigma$ level for the entire day-night times up to 03 May 2019. From 04 May onward the signal amplitudes came back to their normal

variation. As can be seen from the first panel of Fig. 4, ‘local lightning’ was more on 03 May as the cyclonic storm moved toward CUB with more thunderclouds. This can also be seen from the radar image shown in Fig. 4b with the squall line near the receiver. Total lightning was more on 01 May and 03 May compared to 02 May associated with the Fani. But whether there was ‘local lightning’ or ‘distant lightning’, sferics amplitudes at CUB increased all times from their normal values at all three frequencies.

Thus the ionospheric propagation of sferics originating from distant lightning in CUB resulted in a constructive interference among various waveguide modes causing an increase in field intensity of sferics. Constructive or destructive interference of the sub-ionospheric signals depends on the propagating distance. We have observed positive effects in CUB and negative effects in CHB due to ionospheric propagation effects. Nevertheless, the observations at two sites suggest that monitoring of signal amplitudes from sferics can give important information about the cloud-to-ground lightning associated with tropical cyclones and can be used to assess the electrical structures of the tropical cyclones as well.

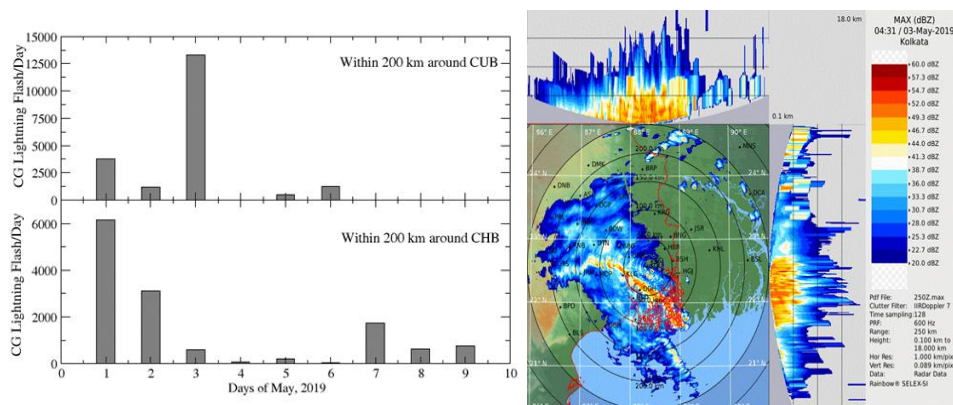


Fig. 4: Cloud-to-ground (including +CG and -CG) lightning flash count per day (left) from 01 May to 10 May 2019 within 200 km of the receiver CUB and CHB. The lightning on 01-03 May 2019 was associated with the ESCS Fani at CUB and was most on 03 May in the region. (Right) Reflectivity (Max dBZ) from the IMD Doppler Radar at Kolkata on the landfall day of 03 May 2019 showing the squall line formed on the same day associated with the cyclonic storm.

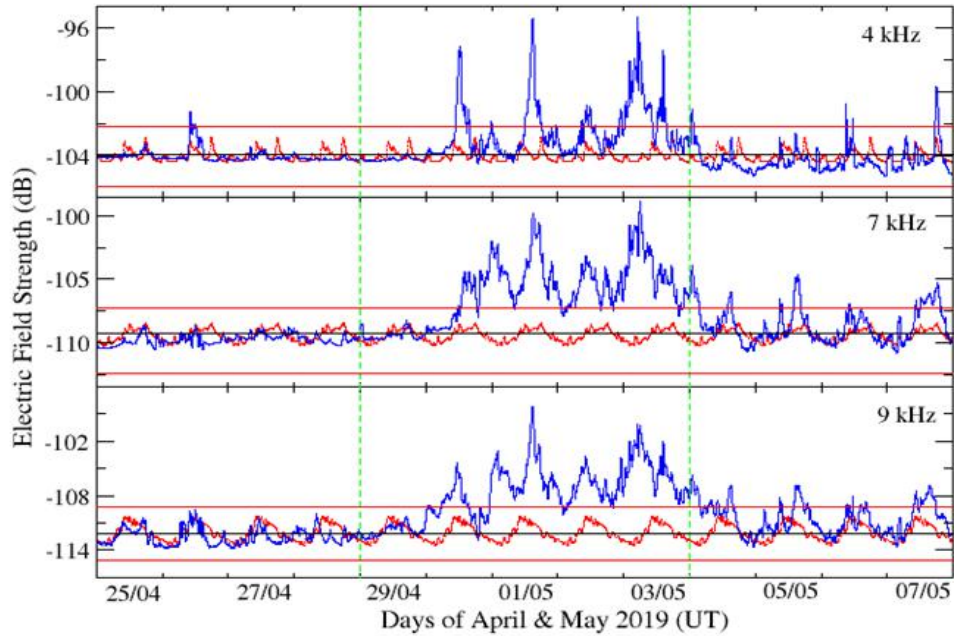


Fig.5: Same as Fig. 2 but for the CUB receiver. In general, minimum in diurnal variation was observed around ~4-5 UT (9:30 LT) and maximum was observed around 12-14 UT (17:30-19:30 LT) for any normal day.

3.2 CASE OF AMPHAN

Amphan was the first Super Cyclone (SuCS) after the Odisha SuCS (1999) over the North Indian Ocean region and originated from a low-pressure area in a near-equatorial region that converted into a Cyclonic storm (CS) in the evening of 16th May and intensified further into a SuCS on 18th May 2020 with a peak wind speed of 260 km/h (1-minute sustained) around 12:00 UT. Thereafter, it continued to be over the Bay of Bengal and made landfall over the West Bengal coast around 10:00 to 12:00 UT on 20 May with 1-minute sustained winds of 155 km/h. Landfall caused large devastation in the coastal regions of West Bengal and Odisha, India. On 21 May at around 1800 UT it weakened into a low-pressure area over Bangladesh.

The two VLF receivers at CUB and CHB were also monitoring the cyclone, but unfortunately, the system at CUB did not save the text file which contained the data of May 2019 due to some computer/software failure except the electromagnetic spectrum in the entire VLF range. Fig. 6 presents the diurnal variation of the field intensity of VLF sferics at three frequencies 4 kHz (upper panel), 7 kHz (middle panel), and 9 kHz (lower panel) respectively from 11 May to

27 May 2020 for CHB station. The duration of the Amphan is shown by the two green dashed lines. The reference signal at each frequency is shown by the red curves obtained by averaging the signal amplitudes of seven quiet days before the cyclone. Blue curves are actual sferics signal.

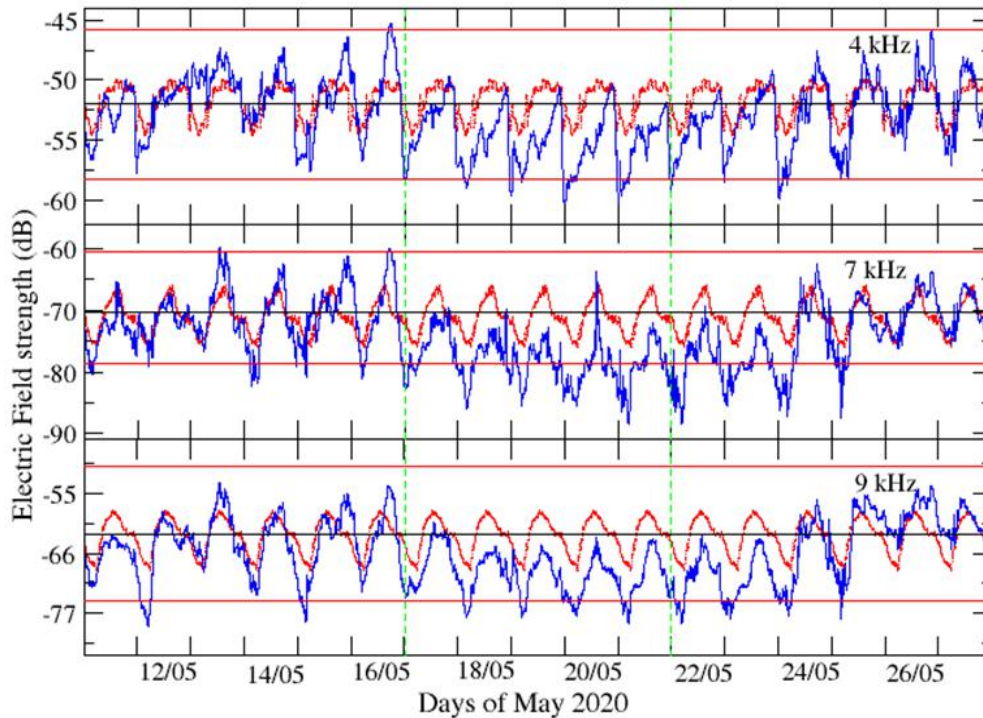


Fig. 6: VLF sferics amplitude (dB) from 11/05/2020 to 27/05/2020 received at CHB (solid blue curve), compared with the variable mean amplitude (red dotted curve) and Amm (black solid horizontal line). Two red solid horizontal lines represent $\pm 3\sigma$ range. Upper panel represents the sferics amplitude at 4 kHz, middle panel is for 7 kHz and lower panel is for 9 kHz. Two green dashed vertical lines indicate the period of SuCS Amphan.

It can be seen from the figure that the entire diurnal variations at each frequency were much lower than the mean signal from 17 May to 23 May 2020. In this case, the maximum deviation can be seen on the landfall day 21 May and the 7 kHz signal responded most during the period. We plot the 'local lightning' near the receiver at CUB and CHB in Fig. 7 which shows the absence of a significant amount of 'local lightning' during the cyclone period 17-22 May 2020. The day when significant 'local lightning' occurred near the receiver, field intensity of sferics at each frequency enhanced from their mean level (as can be seen for 13-16

May). The number of lightning associated with the Amphan increased significantly from 17 May which can be considered as ‘distant lightning’ as the sferics signals traveled ~1000-3000 km to reach CHB.

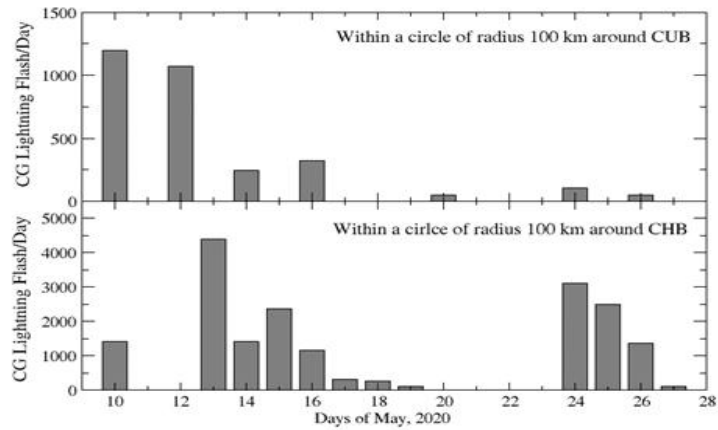


Fig. 7 - Cloud-to-ground (both positive CG and negative CG) lightning flash per day within the 100 km radius of the receivers at CUB (upper panel) and CHB (lower panel).

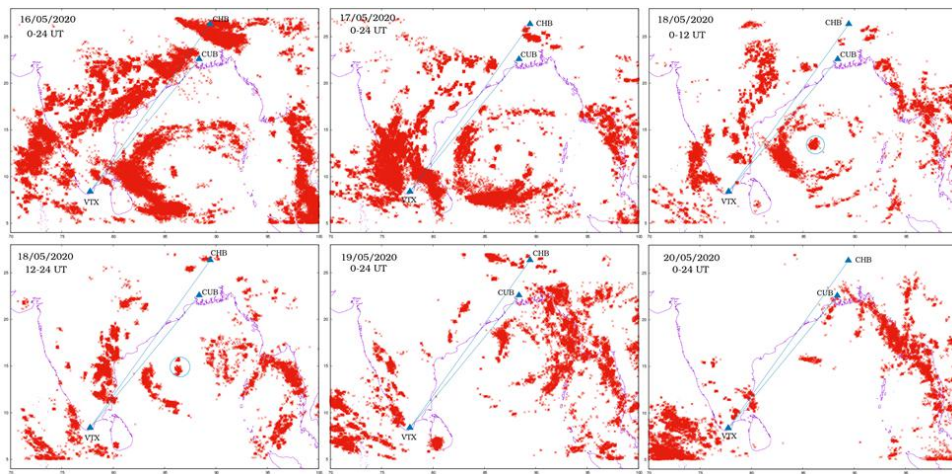


Fig. 8 - Distribution of Cloud-to-ground (includes both +CG and -CG) lightning flashes from 16 May to 20 May associated with SuCS Amphan. Lightning count was the highest around the cyclone eye during peak intensity period. The eye-wall, inner rain band and outer rain band are clearly visible when lightning were grouped into 6 hour interval such as shown for 18 May. Note that the size of eye-wall, inner rain band also the lightning counts were much larger for Amphan than were for the Fani

The distribution of all cloud-to-ground lightning associated with the Amphan from 16 May-20 May 2020 is shown in Fig. 8. The encircled lightning was associated with the Amphan eye. When the sferics originated from ‘distant lightning’ associated with the Amphan reached the receiver at CHB via earth-ionosphere waveguide destructive interference reduced the sferics amplitudes at all frequencies. This was also seen in the case of ESCS Fani of 2019 at CHB. Thus at CHB, it is the ionospheric radio propagation characteristics that caused the reduction in signal amplitudes for sferics signal. As mentioned earlier, there was no data due to computer failure at CUB during this time we could not check the variations of the field intensity of the sferics associated with the Amphan. However, we have the hourly spectrogram for the entire range during the above period. Fig. 9 shows such spectrograms from 16-20 May 2020.

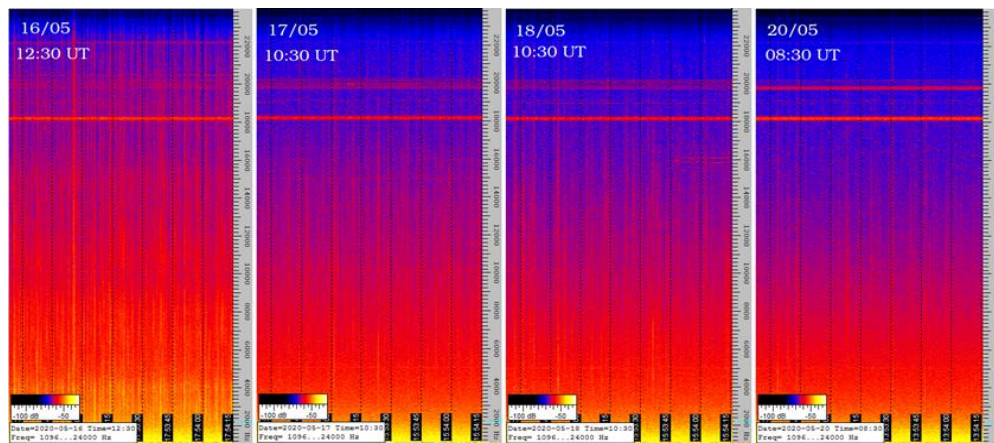


Fig. 9 - Spectrogram recorded at CUB during Amphan in the VLF range. The signal at 18.2 kHz (prominent horizontal line) is the signal of Indian VTX transmitter.

There was ‘local lightning’ around CUB on 16 May (see in Fig.7 upper panel) which could be associated with the Amphan and we see from Fig.8 that sferics dominated the VLF range increasing the electromagnetic noise floor. Similarly for 17-18 May, the electromagnetic noise floor was elevated due to sferics originated far from the receiver (see in Fig. 8). Electromagnetic noise due to the sferics was relatively low on 20 May before the computer stopped working due to the arrival of the storm associated with the Amphan in Kolkata. Although we have no data for diurnal variations for the sferics field intensity, we can conclude from the spectrogram records that the amplitudes of the sferics signals have increased during the Amphan as it also behaved during the ESCS Fani in CUB.

4. SUMMARY AND CONCLUSION

In this paper, we explore the possibility of monitoring the electrical characteristics of tropical cyclones using VLF sferics recorded at two places. This is the first work of its kind over the North Indian Ocean associated with ESCS and SuCS. Both enhancement and reduction in amplitudes of the VLF sferics are observed during cyclone days. Our unique observations are summarized here:

- Amplitudes of VLF sferics at three frequencies (4 kHz, 7 kHz and, 9 kHz) have deviated significantly from mean reference level during cyclone days. A large increase in amplitudes observed at CUB both during 'local lightning' and 'distant lightning' events. On the other hand, reduction in amplitudes is found at CHB during 'distant lightning' events and enhancement in amplitudes is observed during 'local lightning' events.
- The response of sferics amplitudes is greater i.e. the enhancement is much stronger at CUB than at CHB. On the other hand, sferics amplitude at 7 kHz seems to respond strongly with lightning at both places.
- The diurnal amplitude variation of sferics at each frequency was affected for 6-7 days during Amphan. On the other hand, the diurnal variation was affected for 4 days at CUB and 2 days at CHB during Fani. This is because of more lightning associated with the SuCS Amphan compared to ESCS Fani.
- The distribution of CG lightning associated with the cyclones is also presented. The size of the eye-wall, inner rain band, and also the lightning counts were much larger for Amphan than that were for the Fani. More lightning was observed during the peak intensity phase in the vicinity of cyclone eye for SuCS Amphan than ESCS Fani.

We have pointed out important aspects of sferics propagation in the earth-ionosphere waveguide. From the observations and results, the following conclusions are made:

- Lightning activity near the receivers (within 100-200 km radius) always increases the sferics amplitude significantly because of dominant direct VLF waves coming from the lightning discharge. In this case, amplitude enhancement is proportional to the number of CG lightning flash around the receiver.

- An increase in ‘distant lightning’ activity does not always increase the amplitudes of the sferics signals. In this case, sferics propagate a large distance (>1000 km) within the EIWG before reaching the receivers. Depending on the propagation distance and ionospheric conditions, modal interference may change from place to place and may result in increase in amplitudes at one place (such as CUB in our case) and a decrease in amplitude at another place (such as CHB).
- It is now well established that cyclonic storms perturb the ionosphere either through gravity waves coupling or through electromagnetic coupling. We believe that different modes of the sferics signals at CHB from ‘distant lightning’ interfere destructively during the maximum phase of the cyclones due to the propagation through ‘cyclone-perturbed’ earth-ionosphere waveguide.
- This type of investigation is important to know the behavior of VLF sferics with respect to electrical structure and distribution of lightning associated with cyclonic storms. It is also possible to determine any ionospheric modification caused by the increase in lightning activity during cyclonic storms using VLF sferics propagation, recorded by a distant receiver or by a network of receivers, as one of the diagnosis tool.

ACKNOWLEDGEMENTS

Authors express their deepest gratitude for the financial support provided by Science & Technology and Biotechnology Department of Govt. of West Bengal, India (Sanction Memo no. 917(Sanc.)/STBT-11012(20)/42/2019-ST SEC). Authors also acknowledge the Earth Networks Total Lightning Network (ENTLN) and Indian Meteorological Department (www.imd.gov.in) for the production of the data used in this research effort. VLF data can be obtained from Near-Earth Space and Atmospheric Observatory (root.nesao@gmail.com).

REFERENCES

- [1] V. A. Rakov and M. A. Uman, *Lightning: Physics and Effects*, Cambridge Univ. Press, Cambridge, U. K. (2003).
- [2] V. Rakov, *Electromagnetic methods of lightning detection*, *Surveys in Geophysics*, **34(6)**, 731–753 (2013). <https://doi.org/10.1007/s10712-013-9251-1>
- [3] C. O. Price, O. Pechony, and E. Greenberg, *Schumann resonances in lightning research*, *J. Lightning Res.*, **01**, 1-15 (2007).
- [4] S. A. Cummer, and U. S. Inan, *Modeling ELF radio atmospheric propagation and extracting lightning currents from ELF observations*, *Radio Sci.* **35**, 385–394 (2000). <https://doi.org/10.1029/1999RS002184>.

- [5] H. R. Arnold and E. T. Pierce, *Leader and junction processes in the lightning discharge as a source of VLF atmospherics*, Radio Sci., **68D**, 771–776 (1964).
- [6] A. Guha, B. Trisanu, B. K. De, R. Rakesh, and A. Choudhury, *Characteristics of severe thunderstorms studied with the aid of VLF atmospherics over North–East India*, Journal of Earth System Science, **04**, 1013-1021 (2013). <https://doi.org/10.1007/s12040-013-0322-y>.
- [7] B. K. De and S. K. Sarkar, *Regular and seasonal behaviour of atmospheric radio noise field strength (ARNFS) over low latitude station Calcutta*, Meteorol. Atmos. Phys., **61**, 107–114 (1996). <https://doi.org/10.1007/BF01029715>.
- [8] A. K. Sen, A. B., Bhattacharya and S. K., Sarkar, *Very low frequency atmospheric radio noise field intensities*, Arch. Meteorol. Geophys. Bioklimatol., Ser., **A31**, 263–268 (1982), <https://doi.org/10.1007/BF02258038>.
- [9] T. G. Wood and U. S. Inan, *Long range tracking of thunderstorms using sferics measurements*, J. Geophys. Res., **107(D21)**, 4553 (2002). <https://doi.org/10.1029/2001JD002008>
- [10] A. Guha and B. K. De, *Lightning electrical characteristics during tropical summer thunderstorm in north-east India*, J. Atmos. Sol. Terr. Phys., **71**, 1365–1373 (2009). <https://doi.org/10.1016/j.jastp.2009.06.004>.
- [11] A. B. Bhattacharya, S. K. Kar and R. Bhattacharya, *Response of thunderstorm and lightning activity to solar modulation of atmospheric electrification.*, Theor. Appl. Climatol., **58**, 95–103 (1997). <https://doi.org/10.1007/BF00867436>.
- [12] B. B. Goswami, P. Mukhopadhyay, R. Mahanta and B. N. Goswami, *Multiscale interaction with topography and extreme rainfall events in the northeast Indian region.*, J. Geophys. Res., **115**, D12114-D12125 (2010).
- [13] M. R. Chowdhury, S. Biswas, S. Das, A. B. Bhattacharya and J. M. Lichtman, *A study on the spectral pattern of sferics as derived from ELF/VLF radio signal at Techno India University Campus, Kolkata during cyclone 'Roanu'*, International Conference on Computer, Electrical & Communication Engineering (ICCECE), Kolkata, pp.1-6 (2016), <https://doi.org/10.1109/ICCECE.2016.8009562>
- [14] S. S. De, B. Bandyopadhyay, S. Paul, D. K. Haldar, M. Sanfui, B. K. De, G. Chattopadhyay, and A. K. Kundu, *AILA-2009: Its Effects on VLF IFIA and Probable Scientific Explanation.*, Bulg. J. Phys., **38**, 433-477 (2011).
- [15] N. N. Solorzano, J. N. Thomas and C. Bracy, *Monitoring tropical cyclones with lightning and satellite data.*, Eos Transactions, American Geophysical Union". evisa, **99**, (2018). <https://doi.org/10.1029/2018EO092439>.
- [16] F. Wang, X. Qie, D. Wang and A. Srivastava, *Lightning activity in tropical cyclones and its relationship to dynamic and thermodynamic parameters over the northwest Pacific.*, Atmospheric Research, **213** (2018). <https://doi.org/10.1016/j.atmosres.2018.05.027>.
- [17] L. Pan, X. Qie & D. Wang, *Lightning activity and its relation to the intensity of typhoons over the Northwest Pacific Ocean.*, Adv. Atmos. Sci., **31**, 581–592 (2014). <https://doi.org/10.1007/s00376-013-3115-y>

- [18] R. A. Marshall, U. S., Inan and V. S., Glukhov, *Elves and associated electron density changes due to cloud-to-ground and in-cloud lightning discharges.*, J. Geophys. Res., **115**, A00E17 (2010). <https://doi.org/10.1029/2009JA014469>.
- [19] R. L. Bishop and P. R. Straus, *Characterizing ionospheric variations in the vicinity of hurricanes and typhoons using GPS occultation measurements*, AGU Fall Meeting (San Francisco, Dec. 11-15, 2006); EOS Transactions, American Geophysical Union, **87**, SA33B-0276 (2006).
- [20] H. Takahashi, M. J. Taylor, P. D. Pautet, A. F. Medeiros, D. Gobbi, C. M. Wrasse, J. Fechine, M. A. Abdu, I. S. Batista, E. Paula, J. H. A. Sobral, D. Arruda, S. L. Vadas, F. S. Sabbas, and D. C. Fritts, *Simultaneous observation of ionospheric plasma bubbles and mesospheric gravity waves during the Spread-FEx Campaign.*, Annales Geophysicae, **27(4)**, 1477–1487 (2009). <https://doi.org/10.5194/angeo-27-1477-2009>
- [21] N. P. Perevalova and A. B. Ishin, *Effects of tropical cyclones in the ionosphere from data of sounding by GPS signals.* Izv. Atmos. Ocean. Phys. **47**, 1072–1083 (2011). <https://doi.org/10.1134/S000143381109012X>
- [22] E. H. Lay, X. M. Shao, A. K. Kendrick & C. S. Carrano, *Ionospheric acoustic and gravity waves associated with mid-latitude thunderstorms.*, Journal of Geophysical Research: Space Physics, **120**, 6010–6020 (2015). <https://doi.org/10.1002/2015JA021334>
- [23] M. A. Kuester, M. J. Alexander and E. A. Ray, *A model study of gravity waves over Hurricane Humberto*, J. Atmos. Sci., **65**, 3231–3246 (2008). <https://doi.org/10.1175/2008.JAS2372.1>
- [24] A. Rozhnoi, M. Solovieva, B. Levin, M. Hayakawa, V. Fedun, *Meteorological effects in the lower ionosphere as based on VLF/LF signal observations.* Nat. Hazards Earth Syst. Sci., **14(10)**, 2671–2679 (2014). <https://doi.org/10.5194/nhessd-2-2789-2014>.
- [25] S. S. Das, K. N. Uma and S. K. Das, *MST radar observations of short-period gravity wave during overhead tropical cyclone.*, Radio Sci., **47**, RS2019 (2019). <https://doi.org/10.1029/2011RS004840>
- [26] A. Nina, M. Radovanovic, B. Milovanovic, A. Kovacevic, J. Bajcetic, L. C. Popovic, *Low Ionospheric Reactions on Tropical Depressions prior Hurricanes.*, Advances in Space Research, **60**, 8, 1866-1877 (2017). <https://doi.org/10.1016/j.asr.2017.05.024>
- [27] S. Pal, S. Sarkar, S. K. Midya, S. K. Mondal, Y. Hobara, *Low-Latitude VLF Radio Signal Disturbances Due to the Extremely Severe Cyclone Fani of May 2019 and Associated Mesospheric Response.*, J. Geo. Res. Space Phys., **125**, 5 (2020). <https://doi.org/10.1029/2019JA027288>
- [28] B. Das, S. Sarkar, P. K. Haldar, S. K. Midya, S. Pal, *D-region ionospheric disturbances associated with the Extremely Severe Cyclone Fani over North Indian Ocean as observed from two tropical VLF stations.*, Advances in Space Research, **67**, 01, 75-86 (2021). <https://doi.org/10.1016/j.asr.2020.09.018>
- [29] B. Das, A. Sen, S. Pal, P. K. Haldar, *Response of the Sub-Ionospheric VLF Signals to the Super Cyclonic Storm Amphan: First Observation from Indian Subcontinent.*, Journal of Atmospheric and Solar-Terrestrial Physics, **220**, 105668 (2021). <https://doi.org/10.1016/j.jastp.2021.105668>.
- [30] S. Heckman, C. Liu and C. Sloop, *Earth networks lightning overview.*, International Conference on Lightning Protection (ICLP), 2014.